Polymer Nanocomposites with Prescribed Morphology: Going Beyond Nanoparticle-Filled Polymers

Richard A. Vaia • John F. Maguire

1. Introduction

The large variety of plastics available on the market today is the result of blending; that is combining various polymers or by adding micron-scale or larger fillers, such as minerals, ceramics, metals(or even air). Over the last decade, the utility of inorganic nanoparticles as additives to enhance polymer performance has been established and now provides additional opportunities for many diverse commercial applications. Low volume additions(1~10%) of isotropic nanoparticles, such as titania, alumina and silver, and aniostropic nanoparticles, such as layered silicates(nano-clays) or carbon nanotubes, provide property enhancements with respect to the neat resin that are comparable to that achieved by conventional loadings(15~40%) of traditional micron-scale inorganic fillers. The lower loadings facilitate processing and reduce component weight. Most important though is the unique value-added properties and property combinations that are not normally possible with traditional fillers, such as reduced permeability, optical clarity, self-passivation, and flammability, oxidation and ablation resistance. Beyond maximizing nanoparticle dispersion, however, the morphology of these materials is many times uncontrolled, yielding isotropic nano-filled systems, not necessarily spatially '*engineered, designed and tailored*' composite materials.

This review article will endeavor to "look-over-the-horizon" at the challenges and opportunities in providing the toolbox to direct polymer nanocomposite morphology *in the bulk*, that is deliver "nanocomposites-by-design". Among the many challenges as PNCs move beyond commodity plastic applications, precise morphology control is paramount. Random arrangements of nanoparticles will not provide optimized electrical, thermal or optical performance for many potential hightech applications, such as dielectric under-fills for electronic packaging, printed flexible electronics, engineered aerospace structural components, reconfigurable conductive adhesives and optical gratings to just mention a few.

Specifically, we will focus on the methodologies to control the arrangement and distribution of dispersed, preformed nanoparticles beyond uniaxial alignment(D_∞ and C_∞). After a brief summary of the current status of PNCs(*Background*) and a discussion emphasizing the opportunities afforded by the ability to control nanoparticle hierarchy (*Going Beyond Filled Systems*), two general approaches to this challenge are explored, namely: external-in (*Directed Patterning of Nanoparticle Dispersions*) and internal-out (*Mesophase Assembly of Nano Particles*). Examples from the literature are used to highlight the

Richard A. Vaia

is the Lead of the NanoMaterials Strategy Group and Chair of the NanoScience and Technology (NST) Strategic Technology Team at the U.S. Air Force Research Laboratory (AFRL). His research group focuses on polymer nanocomposites, photonic technologies and their impact on developing adaptive soft matter. He received his PhD degree in materials science and engineering at Cornell University in 1995 and was a distinguished graduate from Cornell 's AFROTC. His honors and awards include the Air Force Outstanding Scientist (2002), MRL Visiting Professor at University of California Santa Barbara, Air Force Office of Scientific Research Star Team (2003-2005; 2005-2007) and the Outstanding Engineers and Scientists Award (2006) from the Affiliate S ocieties Council of Dayton. Rich serves on the editorial board of Chemistry of Materials, Member -at-Large for the Division of Polymeric Materials Science and Engineering of the American Chemical Society, and has authored over 75 peer -reviewed papers and patents.

Polymer Nanocomposites with Prescribed Morphology: Going Beyond Nanoparticle-Filled Polymers
Richard A. Vaia and John F. Maguire, Materials and Manufacturing Directorate, Air Force Research Laboratory, Wright-Patterson AFB, Dayton OH e-mail : richard.vaia@wpafb.af.mil

potential and issues and interested readers are encouraged to further explore the literature surrounding these examples for additional information. These examples are by no means intended to be inclusive. A collection of efforts that demonstrate the potential(explicitly or implicitly) is rapidly growing at the intersection of chemistry, physics, materials science and biomaterials, including those highlighted here, as well as others, such as backfilling of sacrificial templates or in-situ nanoparticle formation within a mesophase.

2. Background

Polymeric Nanocomposites(PNCs) have been an area of intense industrial and academic research for the past 15 years. No matter the measure-articles, patents or R&D funding-worldwide efforts in PNCs have been growing exponentially. For example, the total number of hits for "polymer" and "nanocomposite" on SciFinder(Chemical Abstract Service(CAS) of the American Chemical Society) from 1988 to 2005 is higher than 9400, where the yearly number has approximately doubled every two years since 1992.[1] Recent market surveys have estimated global consumption of PNCs at tens of millions of pounds(~$250M), with potential annual average growth rate of 24% to almost 100 million pounds in 2011 at a value exceeding $500~800M.[2-4] Major revenues are forecast from large commercial opportunities, such as automobile, coatings and packaging, where lower cost, higher performance resins would improve durability and design flexibility while lowering unit price. In light of global polymer production, which from oil alone exceeds 200~450 billion pounds annually, nanoparticle additions to plastics affords one of the commercially largest and diverse near-term applications of nanotechnology.

Since the first reports in the early 1990s[5-10] the term 'polymer nanocomposite'(PNC) has evolved to refer to a multi-component system, where the major constituent is a polymer or blend thereof, and the minor constituent exhibits a length scale below 100 nm. As such, the term is sometimes used as a synonym for inorganic-organic hybrids, molecular composites, or to encompass mature commercial products, such as filled polymers with carbon black or fumed silica. The numerous reports of large property changes with very small(<5 vol%) addition of nanoparticles have fueled the view that nanoparticle addition to polymers delivers huge dividends.

Given the extensive variety of nanoparticles now commercially accessible(clays, carbon nanotubes, quantum dots, metals, silica, titania, zirconia, various oxides, etc.,), the potential combinations of polymers and nanoparticles, and thus the tailorability of the property suite, is essentially endless. The diversity in scientific investigation, technology advancement, processing innovations, and product development is staggering. A significant number of excellent review papers(e.g. clays[11-18] and carbon nanotubes[17-21]) and books[22-25] are available that chronicle and summarize the status of various nanoparticle-polymer combinations and the broad scientific and technological challenges still to be overcome.

Arguably, the goal for the vast majority of these investigations is to achieve increased thermo-mechanical performance through dispersion at the single-particle level. The resulting PNCs are treated much as an isotropic, filled polymer. Thus from the historic perspective, nanocomposites

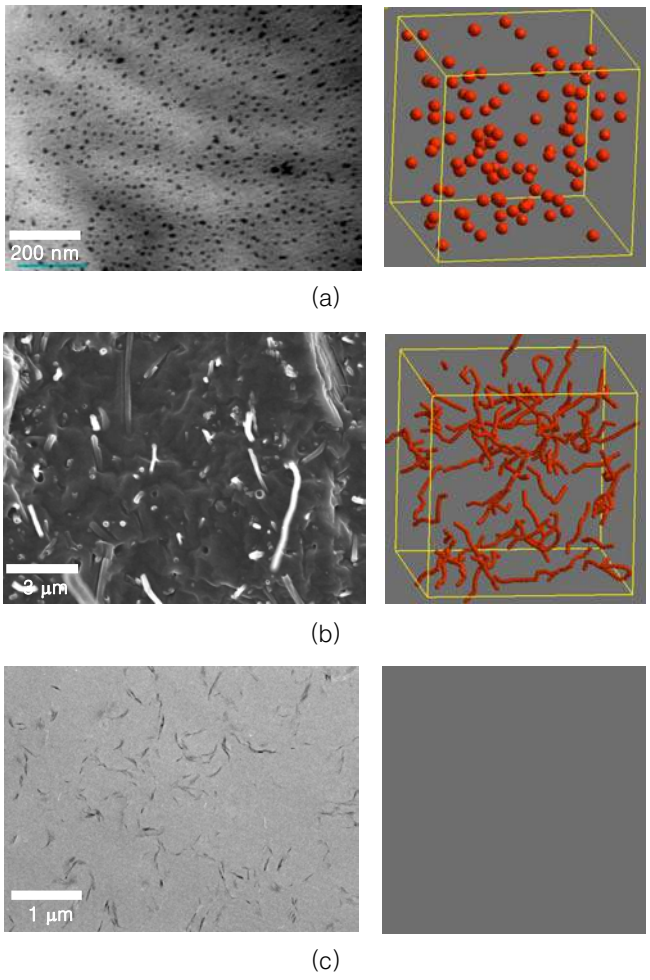

Figure 1. Representative polymer nanocomposite morphologies exhibiting random dispersion of spherical (0D), rod-like (1D) and plate-like (2D) nano-fillers. (a) Spherical: CdSe/ZnS quantum dots with carboxylic acid surface functionality(Evident Technologies) dispersed at 5×10^{15} particles per cm^3 in a recombinant silk-elastin protein (MW 70,000),[26] (b) Rod: 5 wt% carbon nanofibers (Applied Science, Inc) dispersed in thermoplastic polyurethane;[27] and (c) Plate: 3 wt% organically modified montmorillonite(Cloisite 30A) in Epon 862/W cured epoxy.[28]

today are really nanoparticle-filled plastics, **Figure 1**.[26-28] The use of the moniker '*composites,*' though, invokes strong parallels to traditional fiber-reinforced composite technology and the ability to spatially '*engineer, design and tailor*' materials performance for a given application. The pay-off of these manufacturing technologies is exemplified by the incredible material advancements that enable current aerospace systems, both military and civilian. Current processing and fabrication approaches for PNCs fall well short of this fabrication and design capability.

3. Going beyond Filled Systems

Performance enhancements of polymer nanocomposites capitalize on advantages afforded by up to a three orders of magnitude spatial refinement of morphology relative to traditional micron-scale filled polymers and composites. This contrasts nanotechnology in electronics, optics and data storage, where the nano-scale provides access to new physical processes based on quantum phenomenon. Many discussions considering to the implications and physical manifestation of this refinement of PNC morphology can be found in the literature.[29-33] For polymers, many bulk properties are related to the size to the polymer chain, which is characterized by the radius of gyration, R_g(~1-10 nm). The dominating length-scale of the morphology becomes critically important as the dimensions of particle and polymer, as well as the interfacial curvature and inter-particle distance, become comparable. At this point, the propensity of interface and cooperativity between particles dominate macroscopic properties. Strong fundamental parallels can be drawn with efforts on thermal-mechanical characteristics of ultra-thin films of polymers[34,35] or of fluids confined within nanopores.[36] Schadler and coworkers recently provided strong experimental evidence for these parallels through the depression of glass transition temperature in silica filled polystyrene.[31]

For the final material performance though, the extent, spatial arrangement and ordering of the constituents is as important, if not more so, than simply the degree of refinement of the morphology or the role of the interface region on polymer conformation and dynamics. For example, morphology hierarchy is well acknowledged in the processing(injection molding, casting, etc.) of semicrystalline polymers and polymer blends where macroscopic variations, such as skin-core and fountain-flow patterns, arise from specific processing geometry and impact final part design and performance. Comparable processing issues also ultimately determine the utility of many high performance liquid crystalline polymers. For current nanoparticle-filled products, the hierarchy of morphology is even more important than comparable microns-scale filled polymers due to the extreme aspect ratio of many nanoparticles, such as exfoliated clays and carbon nanotubes. Kojima, Usuki and coworkers were one of the first to document and discuss the impact of processing conditions on the fine structure of PNCs.[37,38] They demonstrated that the relative orientation of montmorillonite layers and the concomitant impact on nylon 6 crystallites varied with distance from the sample surface. **Figure 2** summarizes x-ray diffraction studies of an injection molded bar of Nylon 6-montmorillonite nanocomoposite showing that the orientation of montmorillonite and polymer crystallites reflects the filling pattern of the mold. Similar observations are now common in the PNC literature. More recently, Curliss noted the substantial role of the fiber mat in globally templating the alignment of montmorillonite layers during vacuum assisted resin transfer molding(VARTM).[39] Comparison of bulk PNC epoxy to reinforced composite with PNC epoxy matrix indicated that this templated local alignment along the carbon fiber axis was beneficial. Unanticipated improvements of transverse and axial strength in the final fiber-reinforced structure were attributed to the

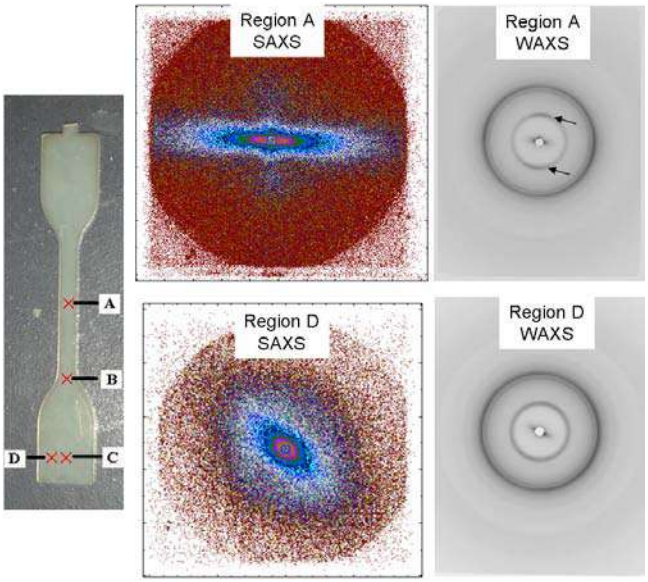

Figure 2. Example of the impact of processing on macroscopic distribution of local morphologies in PNCs. Small angle and wide angle x-ray scattering(SAXS and WAXS) patterns from injection molded nylon 6/montmorillonite nanocomposites reflecting alignment of local structure.[16] The neck region(A in optical picture of the sample) contains highly aligned, well-dispersed montmorillonite layers, as indicated by the oriented streak in SAXS. A weak peak on the meridian of the WAXS patterns arises from well oriented γ-phase crystal lamellae(see arrows). Within the base region(Region D), the montmorillonite layers reflect the fountain flow pattern of the injection molding. The polymer crystallites are not highly aligned, however, as indicated by the more uniform azimuthal scattering in the WAXS pattern from region D.

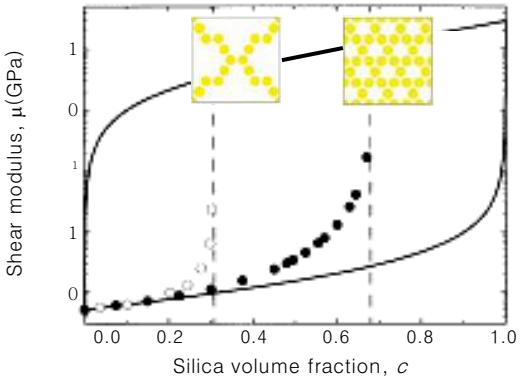

Figure 3. Numerical results obtained by Gusev et al[40] for honeycomb and web-like packing arrays of silica particles(E=70 GPa, ν=0.2) in an elastomer matrix(K=1 GPA, G=0.0005 GPa) demonstrating the impact of controlled morphology on enhancing mechanical properties of a composite. The two solid lines give the predictions of the Hashin-Shtrikman variational bounds. The vertical dashed lines show the maximum packing density that can be achieved assuming web-like and honeycomb packing arrays of identical cylindrical fibers.

alignment of the montmorillonite along the carbon-fiber surface.

Modeling efforts to establish structure-performance correlations further support the need for more refined processing techniques. Reports predict huge dividends in mechanical, barrier and electrical performance if processing could prescribe precise spatial arrangement of nanoparticles. For example, Gusev *et al.* showed that comparable shear moduli could be obtained at only half the volume fraction of particles if a web-like morphology could be generated rather than random or hexagonal arrangement, **Figure 3**.[40] Additional work by Gusev and coworkers on barrier properties[41] and the coefficient of thermal expansion(CTE),[42] and by Boyce *et al*[43] and Balasz et al[44] on mechanical reinforcement further point to the importance of nanoparticle arrangement in achieving maximum effect at minimum filler loading. Using continuum mechanics, Kumar et al examined the elastic constants of single wall carbon nanotube(SWNT) ropes and fibers and showed that shear moduli of the fiber drops precipitously as the width of the uniaxial orientation function of the SWNT increases; upwards of *2 orders of magnitude* for 10~20% disorder at larger fiber diameters.[45] This sensitivity to deviations from perfect order, and its implications to fiber spinning, parallels that known for high performance rigid-rod polymer fibers. Very recently, Forest and coworkers considered anisotropic geometric percolation of high-aspect-ratio rod ensembles dispersed in a viscous solvent and subjected to controlled rheological flows.[46] Results indicated that the spanning dimension of

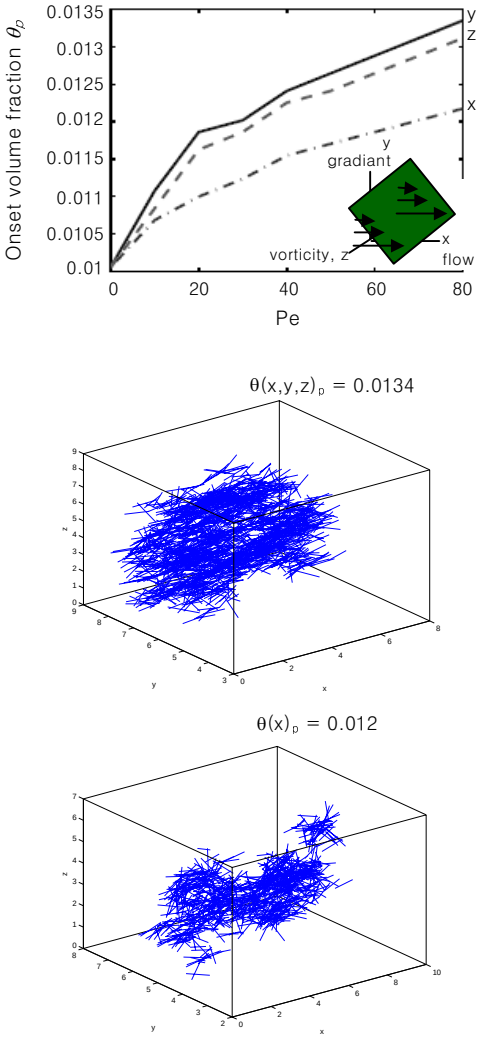

Figure 4. "Percolation phase diagram" of anisotropic percolation thresholds showing the relation between the onset volume fraction θ_p(percolation threshold) and normalized shear rate Pe, for monodisperse rods of aspect ratio 50.[46] The orientational probability distribution function (PDF) of the rods were derived from Doi-Hess theory for flowing rigid-rod macromolecules in a viscous solvent. Representative critical spanning percolation cluster at Pe = 80 corresponding to (top) 3D percolation (θ_p=0.0134) with percolating paths spanning the gradient (y), vorticity (z) and flow (x) direction, and (bottom) 1D percolation(θ_p=0.012) with percolating path only spanning the flow (x) direction.

the percolating cluster can be controlled using a combination of volume fraction and shear rate. Percolation phase diagrams result, in which shear rate produces transitions between 3D, 2D, and 1D percolating clusters, as well as the loss of percolation at a given volume fraction, **Figure 4**. Numerous applications, including smart materials, piezo- and pyro-resistive sensors and actuators, are enabled by the production of films with anisotropic conductivity arising from controlling the structure of the percolation network.

What is the status then of processing techniques that

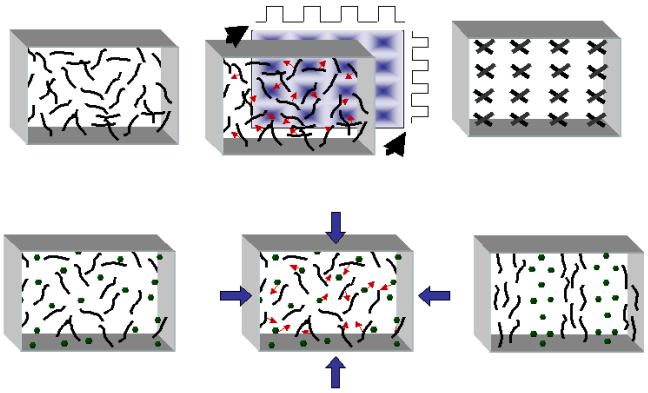

Figure 5. Schematic representation of the two general approaches to control nanoparticle distribution and arrangement beyond random order: external–in (top) and internal–out (bottom). For external–in, *directed patterning of nanoparticle dispersions (DPND)* relies on the creation, by an external means, of a multi–dimensional morphology directing potential (top center: graded background contours), such as a spatially varying field (depicted above) or susceptibility within the material. Imposing this complex field on the sample (top–center) transforms a random distribution to a prescribed, ordered construction due to mass flow of nanoparticles (arrows) to minimize the potential energy of the system within the externally applied field. For internal–out, *mesophase assembly of nanoparticles (MANP)* relies on the ability to tailor interparticle interactions, both particle–particle and particle–matrix, to result in thermodynamically stable (and defined) mesophase. The phase behavior of the system may be modulated(bottom center) by uniform changes in the systems intrinsic (pressure or temperature) or extrinsic (number density or entropy) thermodynamic parameters. In contrast to the externally patterned potential applied for *DPND*, changes in particle organization in *MANP* occur in response to a uniform change in the system's environment.

will provide a feedback to, and a demonstration of, these insights? It seems clear that more than uniaxial control of rods and plates is necessary.

Ultimately, two general approaches to this challenge, paralleling nanofabrication concepts, are emerging, namely: external–in(top–down) and internal–out(bottom–up), **Figure 5**. For external–in, *directed patterning of nanoparticle dispersions(DPND)* relies on the creation, by an external means, of a multi–dimensional morphology directing potential, such as a spatially varying field or susceptibility within the material. This transforms a random distribution to a prescribed, ordered construction. For internal–out, *mesophase assembly of nanoparticle(MANP)* relies on the ability to tailor interparticle interactions, both particle–particle and particle–matrix, to result in thermodynamically stable(and defined) mesophases. The possibilities for higher order structures are bolstered by the continuing successes in the reproducible production of nano– spheres, fibers, plates and other geometries with manufacturing tolerances that approach the current norm of micron–scale fibers, colloids and films(<1%).[47–52] These will provide nanoscale building–blocks approaching the precision of molecules, macromolecules and biomacro–molecules and thus access to the associated complex phase space.

4. Directed Patterning of Nanoparticle Dispersions

The ability to uniaxially align nanoelements, both plates and tubes, using external forces and gradients has been extensively demonstrated. Approaches include sedimentatio,[53] spin coating,[54] mechanical deformation(fiber spinning,[55–58] film blowing,[59] injection molding,[60] shear),[61,62] magnetic fields,[63,64] and electrical gradients.[65] One–dimensional, out–of–plane periodicity has also been shown by sequential deposition approaches such as electrostatic or hydrogen bond mediated self–assembly.[66,67]

Much less work has been directed towards establishing robust processing techniques that enable broad tunability of two– or three dimensional structures within the bulk. Creation of multidimensional structures is challenged by how to controllably generate a multi–dimensional, morphology–directing potential within the bulk material. For example, if the control input is mechanical deformation, morphology manipulation will depend not only on the magnitude and gradient of an anisotropic external deformation(all components of the stress tensor) but also on the local distribution of the stress field and on the coupling to, and interplay of, the nanoparticle's shape and mechanical response(buckling, fracture, etc.), surface energies, viscoelastic properties, etc. Extensive efforts on the refinement of two–component polymer blends exemplify the complexity of this specific case.[68]

The following sections highlight four areas which provide an overview of current capabilities. The initial three sections(*Mechanical Deformation, Electric and Magnetic Fields* and *Optical Fields*) discuss the coupling between applied external fields and nanoparticle orientation, distribution and interparticle interactions. The last section (*Multi–component Interfacial Systems*) considers the possibilities afforded by interfacial segregation of nanoparticles in an immiscible blend, and thus templating the nanoparticle distribution to the interfacial regions of the immiscible blend, and subsequent macroscopic manipulation via distortions and refinements of the two–phase morphology.

4.1 Mechanical Deformation

For mechanical deformation, uniaxial or in–plane biaxial arrangement of the nanoparticle and polymer crystallites is common, as noted by the aforementioned approaches. Multi–dimensional control of the morphology by complex

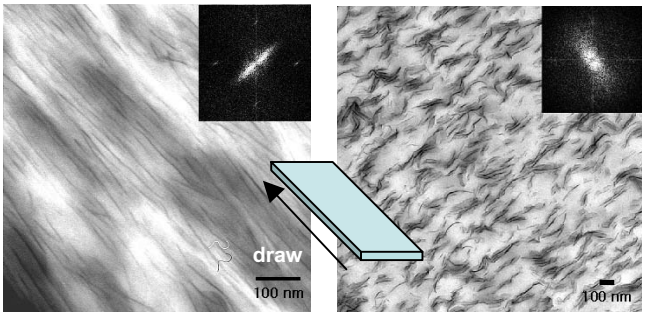

Figure 6. Transmission electron micrographs from Park *et al.*[69] of a biaxially protruded and then drawn film of nylon 6–montmorillonite nanocomposite perpendicular (left) and parallel (left) to the draw direction demonstrating buckling of the nanolayers.

strain fields is rarely reported. However, some reports of using controlled strain inputs to introduce local distortions of the nanoparticle can be found. For example, beginning from quenched biaxially extruded films of nylon-6/ montmorillonite nanocomposites, Park and co-workers observed within zone-drawn films that the montmorillonite layers buckle perpendicularally to the draw direction, analogous to failure of a uniaxially strained sheet of paper.[69] The failure mode appeared to occur for a collection of parallel aluminosilicate layers (2-4) and exhibited a mean spatial frequency, **Figure 6**. This behavior has analogies to shear banding and deformation of uniaxially-aligned lamellar and cylindrical block copolymes.[70-72]

In general, nanoparticle alignment, as well as morphology refinement, depends on the type of imposed flow, whether extensional, shear or mixed.[73] This is analogous to other complex fluids including polymers. Fundamentally, the complexity of the local response to imposed stress or strain not only depends on the interfacial strength, particle size and mechanical characteristics of the constituents, but also on elastic instabilities, such as buckling, of the high aspect ratio nanoparticles, as well as the cooperative response of nanoparticles coupled through overlapping local strain fields. The extent of the latter is many times reflected in a lower volume fraction for mechanical percolation ($\varepsilon \rightarrow 0$) than electrical percolation. Systematic exploration of this complex processing space to produce hierarchical structures by inducing particle orientation and particle deformation, as well as transferring insights from shear thinning (pseudo-plastic) and shear thickening (dilatant) fluids, is still in its infancy.

4.2 Electric and Magnetic Fields

The morphological origins of stiffening of rheological fluids, such as electro- (ER) and magneto- (MR), provide a perspective on the possibilities for externally applied, spatially patterned, electrical and magnetic fields for complex PNC fabrication. Under the electric field, particulate additives, such as oxides or metals, reversibly form fibrous structures within the non-conducting fluid. These controlled aggregates are parallel to the applied field and can increase the viscosity of the ER fluid by a factor of up to 10^5.[74] Similar morphologies are found for magneto-rheological fluids where particle-particle interactions, which arise from induced magnetic dipoles, lead to chaining and subsequently long-range, periodic ordering of the particle chains parallel to the lines of magnetic flux.[75] Gradients of magnetic or electric fields also generate lateral forces that can be used to pattern nanoparticles. For example, electrophoresis approaches have been extensively developed in the biological community for nucleic acid and protein purification[76] and di-electrophoresis for nanofabrication to align particles between electrodes or trap nanoparticles in specific regions.[77] Also, local instabilities at the interface between two fluids can be enhanced with applied electrical or magnetic fields, providing a means to control the growth of certain Fourier components of the spatial frequency of the composition modulation.[78,89]

Even with these proven successes though, direct application to large scale PNC production is challenging. Generating reconfigurable gradients in 3-dimensions with micron (or sub micron) features requires complex tooling with reconfigurable, patterned electrodes. As particle size decreases, the fields necessary to overcome thermal randomization increase considerably,[80,81] and may approach the break-down strength of the matrix. This drastically limits sample thickness. Also anisoptropic particles (rods and plates) drastically increase the complexity (and predictability) of field response with respect to the more commonly used spherical shapes. Finally, for thermoplastics, high viscosity results in long mass transport times, even over short sub-micon distances. Nevertheless, adaptations of these concepts to PNCs, especially thermosets where order can be 'stabilized' via post- processing polymerization, are now providing intriguing possibilities to move beyond uniaxial alignment.

As an example, Koerner and coworkers[63] exploited the orthogonal magnetic susceptibility of montmorillonites from different mineral deposits to fabricate a three-dimensional morphology composed of orthogonal alignment of aluminosilicate layers using a uniaxial external magnetic field. Depending on the source, montmorillonites exhibit remnant magnetization arising from antiferro- and ferrimagnetic impurities and align with layers parallel or perpendicular to the field, **Figure 7**. Within a few minutes, application of static magnetic fields (1.2 or 11.7 T) induces stable alignment of organically-modified montmorillonites

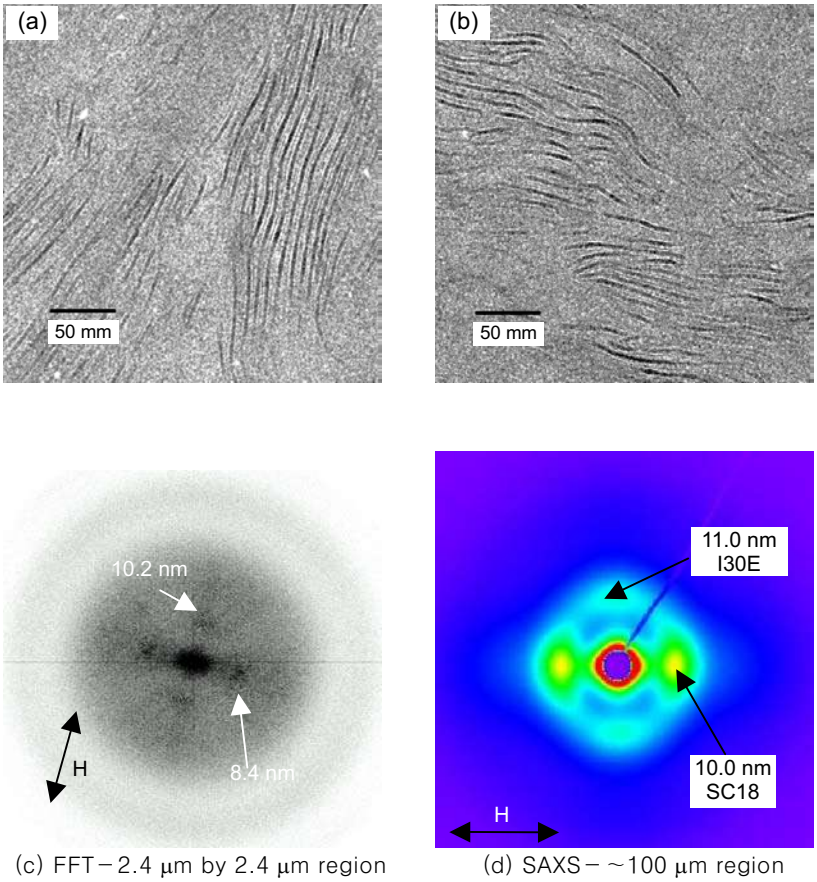

(c) FFT－2.4 μm by 2.4 μm region (d) SAXS－～100 μm region

Figure 7. Magnetic alignment of an equal mixture of two octadecyl ammonium modified montmorillonites (SC18 and NC18) in e poxy(6 wt% total).[63] High resolution transmission electron micrograph of regions of the nanocomposite with a) SC18 layers parallel to, and b) NC18 layers perpendicular to, the applied magnetic field. (c) Digital Fourier Transformation(DFT) of a transmi ssion electron micrograph of a 2.4×2.4 μm area showing correlation peaks arising from the ind ependently aligned montmollinites. d) Small Angle X－ray pattern showing a four－point pattern caused by orthogonally aligned montmorillonite tactoids.

within an epoxy resin at room temperature. Structural relaxation in the absence of the field is orders of magni－tude slower enabling the alignment to be captured during the subsequent cure. This could offer a pathway to a viable manufacturing technology. Thermal mechanical measurements demonstrate that this morphology manipulation impacts the coefficient of thermal expansion (CTE), decreasing CTE by an additional 20～30% in the direction of maximum montmorillonite alignment with respect to that of the isotropic PNC. This example demonstrates that through the use of two or more nanoparticles with different susceptibilities to the externally applied field, the complexities associated with applying non－ uniaxial fields to the sample could be overcome. In support of this concept, aligned arrays along the electric－field direction of binary blends of silver and silver oxide nanoparticles(～8.5 nm) in polymethylmethacrylate film has recently been demonstrated,[82] providing further glimpses at the possibilities for complex internal structures when nanoparticle blends are used. Other reports discussing CNTs in magnetic fields,[83] and electric fields [84] are available. Comparable results have also been reported for electric field assisted alignment of montmorillonite in epoxy.[65] As with dual frequency liquid crystals, frequency－dependent differ－ences in the direction and magnitude of the induced dipole on anisotropic nanoparticles may afford benign tuning of the distribution,[85] however this as yet to be demonstrated.

4.3 Optical Fields

Holographic photopolymerization has also been shown as a viable nanoparticle directing tool, creating periodic, multidimensional arrangements of gold nanoparticles, colloids, layered silicates, TiO_2, ZnO_2, and CdSe,[86－88] In－terference of two or more coherent laser beams within a photo－reactive monomer syrup results in a periodic in－tensity distribution that initiates a self－similar periodic, polymerization process. A higher intensity results in a locally faster polymerization rate. This distribution in poly－merization rate causes a spatially periodic distribution of high molecular weight polymer, which changes over time.

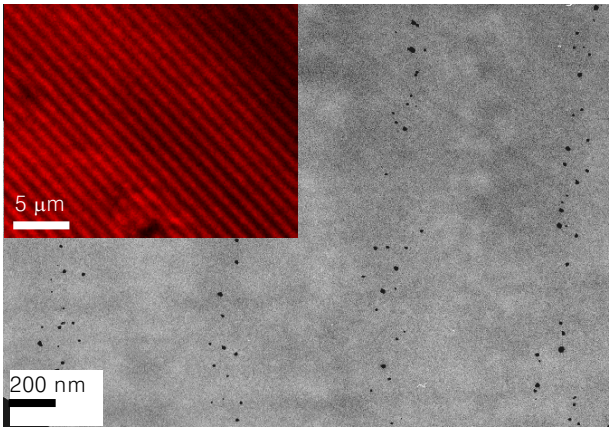

Figure 8. Holographic photopolymerization patterning of gold nanoparticles in an arcrylate resin.[86] Transmission electron micrograph shows a cross-section of planes of gold nanoparticles on an ~450 nm period that are oriented perpendicular to the substrate. The planes of Au nanoparticles span the 10 micron film thickness. The inset shows an optical confocal microcopy image of the surface of the transmission grading formed by these patterned gold nanoparticles.

The temporal evolution of the polymer can locally induce phase transitions, such as demixing, or result in mass flow, which concentrates (or traps) nanoparticles in regions of low (or high) intensity depending on particle size and surface reactivity. **Figure 8** summarizes one such fabricated structure generated using two-beam interference lithography - planes of gold nanoparticles oriented perpendicular to the film surface. More complex structures paralleling those demonstrated for holographic polymer dispersed liquid crystals[89,90] should be possible with four and six beam holography, such planar trigonal and orthogonal lattices with parallel rods, or 3-dimensional cubic or orthorhombic P structures.

4.4 Multi-Component Interfacial Systems

Immiscibility is common in many multi-component systems, both polymers and nanoparticles. Nevertheless, the interface between the immiscible phases affords opportunity for structural organization of nanoparticles. Conceptually, this derives from a common approach to compatibilization of immiscible blends - the addition of a small quantity of a third component that is miscible with both phases (co-solvent), has a surface energy with the two constituents that is less that that between the constituents, or is a structured amphiphile whose sections are miscible with each component respectively.[91] The additive is designed such that segregation to the interface is energetically favorable. The process leads to reduction of the interfacial tension, facilitating refinement of the phase domains; stabilization of the morphology against high stress and strain processing (e.g., in injection molding); and/or enhancement of adhesion between the phases in the solid. The distribution of interfacial regions within the final materials depends on process history and thus provides a means of tailoring the macroscopic arrangement of nanoparticles.

As an example, layered silicates have been discussed as compatibilizers for immiscible polymer blends, and thus demonstrating the potential to sequester at the interface.[92,93] Ahn et al.[92] observed that when a very small amount of organoclay (1%) is added to a PBT/PE blend, the organoclay is located at the interface and the organoclay tactoids are disrupted into thinner tactoids of some tens of nanometers. The presence of organoclay at the interface hydrodynamically stabilizes the blend morphology by suppressing the coalescence of the droplets and also makes the two phase polymer blend morphology more thermally stable. Sequestering montmorillonite at the interface in immiscible polystyrene/polypropylene blends has also been observed.[94]

Pickering emulsions (emulsions stabilized by solid particles) using nanoparticles also offer interesting possibilities. Pickering emulsions are encountered in various natural and industrial processes such as crude oil recovery, oil separation, cosmetic preparation, and waste water treatment. An initially high interfacial energy between 2 phases, such as oil and water, can be decreased by the assembly of the particles at the interface.[95,96] The decrease in surface energy favors the formation of a monolayer of nanoparticles located at the interface, **Figure 9**. Additionally, the relatively low viscosity of the two phases implies the process is highly dynamic, which enables errors (defects) to be corrected rapidly. Russell and coworkers[97] estimated that the stabilization energy, ΔE, decreases as r^2, where r is the radius of the particle. For a water/oil mixture, $\Delta E \sim 10^5$ k_BT for 100 nm particle and $\Delta E \sim 10^1$ k_BT for 1 nm particle. Using CdSe nanoparticles of two different radii (2.7 nm and 4.6 nm), they not only showed CdSe segregation to the interface of an oil-water droplet, but a preferential adsorption of the larger particle. Mohwald and co-workers[98] have created close-packed nanoparticle layers and nano-alloys using Au, Ag or γ-Fe_2O_3. Robust and water dispersible colloidosomes with shells predominantly composed of monolayers of liquid-like, close-packed magnetite nanoparticles has also been created through the gelation of an aqueous phase with agarose after assembly of magnetite nanoparticles at the interface.[99] Binks[100] reported Pickering emulsions using Laponite. Additionally, *N,N*-dimethylformamide-water interface has been used to assemble carbon nanotube-metal nanoparticle composite materials;[101] and aqueous acrylamide (AAm) or 2-hydroxyethyl methacrylate (HEMA) in cyclohexane stabilized by hydrophobic Cloisite 20A (MMT20)

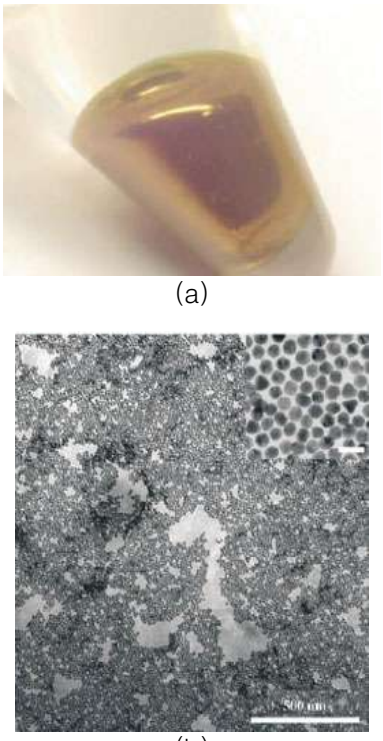

Figure 9. (a) Photograph of the self-assembled Au nanoparticles at the water/toluene interface in a plastic Eppendorf tube from Mohwald *et al.*[98] The tube has been titled such that the colored area corresponds to the water/ toluene interface. (b) TEM image (scale bar 500 nm) of the monolayer of 12-nm Au nanoparticles formed at the water/toluene interface; inset: high-magnification TEM picture (scale bar 25 nm).

lead to polymer-clay nanocomposite latex particles.[102]

The ability to arbitrarily tune the surface properties of the nanoparticle increases the range of potential two-phase systems and morphologies amenable to interfacial sequestration. Recent efforts on mixed surfactant passivation have demonstrated this potential. For spherical particles, mixtures of polymers[103] or organic molecules[104] as passivation yielded nanoparticles with amphiphilic character. In many regards, this concept parallels substantial synthetic work on multiarm miko(heteroarm) polymers.[105,106]

In general multicomponent interfacial systems share many common features with nanoparticle sequestration in mesophases discussed below, differing mostly in the composition and morphology of the polymer media, the density of interfacial area and number density of nanoparticles.

5. Mesophase Assembly of Nanoparticles

Although in principle directed patterning of nanoparticle dispersions provides access to any arbitrary geometry, manufacturing complexities establish practical limits on the thickness and volume of material impacted. These include the excessive time for pattern development in highly viscous media such as polymers, complex external tooling with vibration isolation to maintain structural precision on the submicron scale for non-batch manufacturing, and in some instances(electrical and optical), uniformly achieving the energy density requirements throughout thicker(>100 μm) samples. To complement DPND approaches, the inherent organization derived from a thermodynamically well-defined phase provides an alternative approach to the fabrication challenge. What are the issues then in predicting and accessing these stable mesostructures of nanoparticle assembles in polymers and resins? Do 'phases' of nanoparticles ensembles exist? Are they robust enough to be exploited and utilized?

The phase behavior of hard-body particles has been extensively developed and serves as a starting point from which the properties of nanoparticle-polymer combinations can be considered.[107-109] These idealized systems are defined when the constituent particles interact exclusively through short ranged repulsive forces at the point of particle contact, with no dissipative behavior. For angular particulates whose shape deviates significantly from spherical, entropically-driven excluded volume effects give rise to a wide range of complex ordering and phase behavior including the isotropic-nematic phase transition in liquid crystalline systems.[110] The increased order within the nematic phase increases the number of translational and rotational eigenstates within the system giving rise to a spontaneous entropcially driven transition with negative free energy. The phase behavior of such systems, including rods and discotics(discs), are critically importance to a broad range of technologies such as liquid crystals, high-performance polymers, and biomolecules. Temperature dependence and phases behavior of such systems have been treated theoretically via the early formulations of Flory[111] and Onsager[112] and more recently by de Gennes.[113]

These general topological considerations imply nanoparticle-polymer(or reactive monomer) blends conceptually will show a great structural richness with the possibility to form a variety of exotic phases. Not only do the usual enthalpic and entropic interactions contribute to the chemical potentials but now the topological constraints imposed by size and geometry and the added complexity of surface interactions in what are thermodynamically small systems need to be taken into account. Subtle changes in any of these parameters may tip the balance causing major perturbation on the locus of the curve of equal

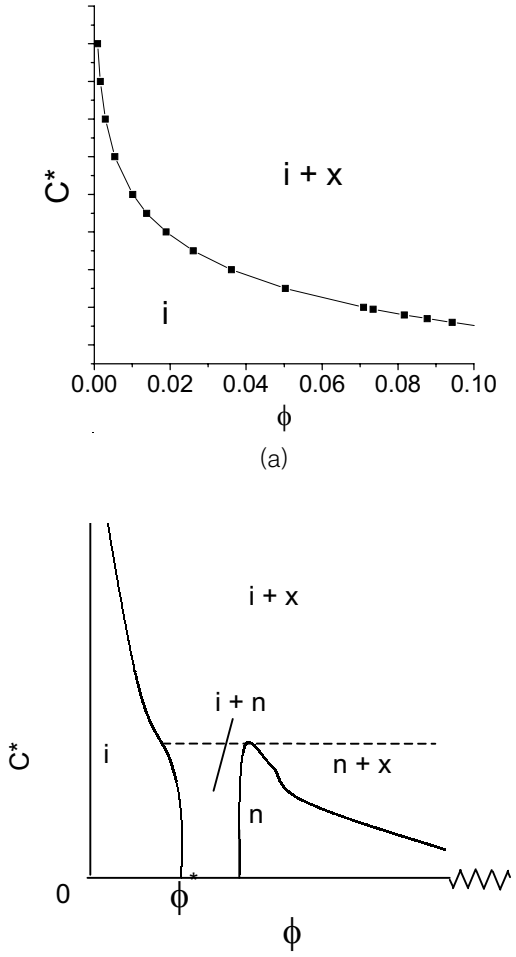

Figure 10. Simplified schematic representations of the phase diagrams for both spherical (a) and rod-like particles (b) of volume fraction, ϕ, dispersed in a polymer of reduced concentration, c*. Spherical particles at low concentration may be highly dispersed with little agglomeration (i). As the concentration rises depletion forces become increasingly important and give rise to agglomeration and phase separation (I+x). As seen in figure (b) the situation for rod-like particles is considerably more complex in that even very small concentrations of rods can give phase separation, extended two-phase coexistence regions and critical phenomena. Orientational correlations result in the formation of a nematic phase (n), which for various volume fraction of rods may be in equilibrium with the lower volume fraction isotropic phase (i) as well as the higher volume fraction aggregate structures (x).

chemical potential, **Figure 10**. For a realistic nanoparticle-fluid system, the extent of the immiscibility window between a low and high volume fraction nanoparticle phase will depend on numerous interrelated contributions to the free energy in addition to the configurational entropy of the constituents. These include intermolecular interactions as well as the relative impact of mixing on the internal degrees of freedom of the constituents (e.g. chain conformation). Additionally, the experimentally accessible region in this phase space will depend on the magnitude of the intensive variables (temperature, pressure, chemical potential, etc.), polydisperity of the constituents, and kinetic considerations such as gelation.

The possibilities afforded by discrete phase behavior of polymer nanocomposite systems may be systematically considered based on how the polymer and nanoparticle are combined to form the constituents of the mixture. To contrast the morphologies created by traditional nanoparticle dispersion, we'll discuss three general types: *nanoparticle-macromolecular systems* comprised of nanoparticles within a complex fluid, such as linear polymers, block copolymers, dendrimers, or liquid crystals; *structured block nanparticles* that are analogous to block-copolymers or macomolecular stars, but where one 'block' or the core is the nanoparticle and the other block or arms is a polymer; and *nanoparticles-nanoparticle systems* containing mixtures of nanoparticles of various sizes and shapes with organic or macromolecular coronas.

5.1 Nanoparticle-Macromolecular Systems

The examination of the phase behavior of nanoparticle dispersion in small molecule or macromolecule medium is rapidly expanding. Approaches range from ordered phases arising from the combination of functional nanoparticles and linear polymer to the use of the phase structure of a block copolymer to template nanoparticle organization.

The similarity between the size of the nanoparticle and the chain results in coupling between the configurations of the constituents (mixing entropy), the internal degrees of conformational freedom of the polymer, and intermolecular and interparticle interactions. This complicates the unambiguous development of models to predict nanoparticle dispersion and phase behavior. Nevertheless, the importance of various factors is beginning to be identified. Schweizer[114,115] as well as Zhong[116] argue for athermal mixtures that there exists oscillatory depletion forces between two hard spheres due to monomer-level packing correlations and the key geometric variable determining nanoparticle aggregation in flexible, high molecular weight polymers is the ratio of particle to monomer diameter. Thus purely athermal mixtures of polymers and nanoparticles are macroscopically phase separated at equilibrium, requiring attractive polymer-particle interactions to achieve miscibility. Recently, simple thermodynamic arguments based on a Flory formulation of the free energy provided a framework to Mackay and coworkers to explain the miscible-immiscible boundary for a C_{60}-polystyrene system.[117] The formulation included distortion of the polymer chain configuration by nanoparticles and a relative increase in accessible surface area of the nanoparticle due

to packing considerations within the nanoparticle aggregate. These factors lead to a maximization of the miscibility window for an optimal nanoparticle size. Finally, Balasz and coworkers combined self-consistent field (SCF) theory with density functional theory to calculate the equilibrium behavior of polymer-clay mixtures, demonstrating the potential to form isotropic, nematic, smectic (lamellar), columnar, crystal, and plastic solid (house-of-cards), as well as a two-phase (immiscible) mixtures.[118] They also examined the impact of surface architecture (tethering density, molecular weight and composition) of polymers end-tethered to the clay surface.[119] Most of these predictions though have yet to be systematically investigated in experimental montmorillonite–thermoplastic systems.

Experimentally, however, the occurrence of complex mesophases of nanoparticle dispersions is well established, although most systems examined to date are in a small molecule medium. For example, experimental phase diagrams have been reported for so-called lyotropic, inorganic liquid crystals.[120] Mesophase formation has been reported for molecular nano-wires, tubes, ribbons and rods ($Li_2Mo_6Se_6$, Imogolite, Nb_2PS_{10}, V_2O_5, Boehmite (γ-AlOOH), Akaganeite (β-FeOOH), Goethite (α-FeOOH)) and nano-platelets and disks (smectic clays, $H_3Sb_3P2O_{14}$, Gibbsite ($Al(OH)_3$), $Ni(OH)_2$), **Figure 11**.[121] Experimental phase diagrams also take into consideration limits due to gelation and aggregation.[122] Alivisatos and coworkers have reported similar behavior for CdSe quantum rods in anhydrous cyclohexane, with anticipated applications for electro-optic devices.[123] Finally, taking inspiration from

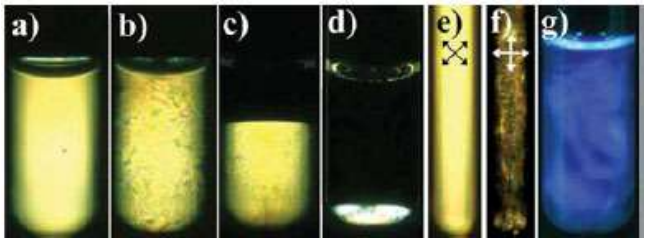

Figure 11. a–g. Phase behavior of aqueous suspensions of $H_3Sb_3P_2O_{14}$ single-layers from Gabriel *et al.*[121] observed between cross polarizers (the isotropic phase appears dark): (a) 2 mL of birefringent gel phase (ϕ=1.98%) (topological defects are so dense that the texture appears homogenous at the scale of the photograph); (b) 2 ml of birefringent fluid phase (ϕ=0.93%); (c) 2 mL of a biphasic sample with an overall volume fraction ϕ =0.65%; (d) 2 mL of a biphasic sample with an overall volume fraction ϕ=0.03%; (e) and (f) magnetically aligned sample observed in a 5-mm NMR tube that has been immersed 10 min in a 18.7 T field at 50 ℃, in two different orientations compared to the polarizer/analyzer system represented by arrows (ϕ=0.75%); (g) sample iridescence (ϕ=0.75%) observed in natural light and due to light scattering by the $H_3Sb_3P_2O_{14}$ layers stacked with a period of 225 nm.

dryjet wet-spinning of liquid crystalline rigid-rod polymers, such as poly (p-phenylene benzobisoxazole) in poly (phosphoric acid), Davis, Adams and Smalley have demonstrated the two-phase 'Flory' chimney between isotropic and nematic phases for solutions of purified single wall carbon nanotubes in superacids, such as oleum.[124] As with the rigid rod polymers, fiber spinning from the nematic phase results in a higher degree of molecular order along the fiber axis. In all of these cases, the mesophase could be captured in a solid monolith by replacing the fluid media with a chemically reactive media, although investigations along these lines are minimal. In general, these morphologies are mostly nematic however, lacking order beyond uniaxial. Nevertheless, these observations establish a parallel to liquid crystal technology, point to the potential for higher order mesophases, and afford yet to be explored opportunities for processing and properties of PNCs.

Paralleling nanoparticle dispersions within a homopolymer or organic media, sequestration of the nanoparticle within one region of a single component complex fluid, such as a block copolymer, has been demonstrated as a relatively facile route to many complex morphologies.[125-128] Fredrickson and coworkers have utilized a self-consistent field theory in which particle coordinates and chemical potential field variables are simultaneously updated in the simulation.[129] The fluid model can contain polymers of arbitrary chemical and architectural complexity, along with particles of all shapes, sizes, and surface treatments. The initial simulations of polystyrene-poly (2-vinyl pyridine) (PS-P2VP) containing PS-functionalized Au nanoparticles paralleled experimental data, **Figure 12**.[125] Additionally, increasing Au-particle density drove the structure from the hexagonal to lamella phase, however the SCFT results (2-dimensional) underestimated the particle density at the morphological transitions. Many experimental analogs to the Au-PS-P2VP system are available including CdSe nanoparticles in PS-P2VP[126] and montmorillonites in polystyrene-polybutadiene-polystyrene (SBS) tri-block.[127] Overall, the architecture and composition of the corona, as well as particle size, provide fine control of the location of the nanoparticle within the preferred domain.[128] By tuning the nanoparticle so that they prefer the interface between the chains of the block, Kramer and coworkers have been able to drive phase transition of the diblock from lamellar to bicontinuous.[130]

5.2 Structured Block Nanoparticles

Contrasting two component systems where one is the nanoparticle and the other is the macromolecule, *structured block nanoparticles* are monolithic structures where

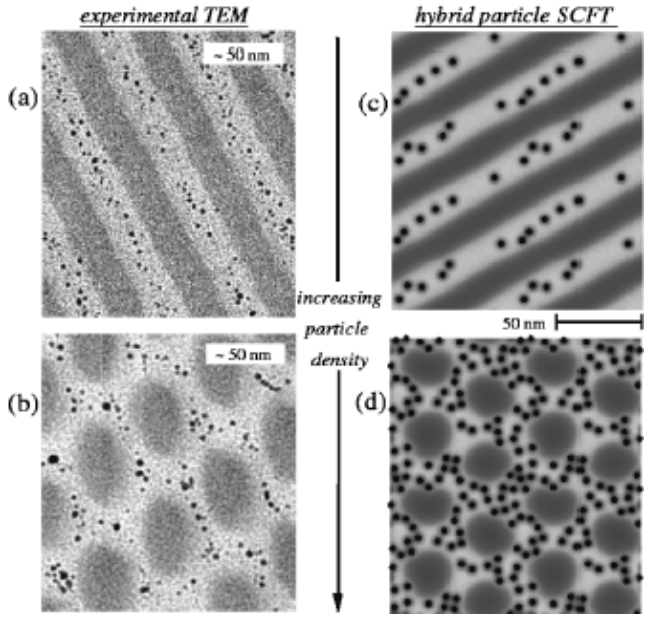

Figure 12. Transmission electron microscopy images from Fredrickson *et al.*[129] of f_{PS}=0.50 PS-P2VP diblock nanocomposite containing(PS)-functionalized Au particles with particle volume fraction (a)=0.10 and (b)=0.35. Total particle size including the PS shell is 2.6 times that of the Au cores seen as black dots in the TEM images. Hybrid particle field simulation results (right column) show monomer volume fractions representing PS(light), P2VP (dark), particles(black). Simulation parameters: f_{PS}=0.5, Flory parameter (χ) for PS-P2VP diblock χ=0.16, λ=0.16, and particle area fraction (c)=0.04 and (d)=0.18. The particle configurations shown are representative of those obtained based on several independent runs for a given nanoparticle density.

the nanoparticle and macromolecule are coupled in a controlled and reproducible fashion. The phase behavior of these structured single components is exemplified by block-copolymers[131] or liquid crystals polymers.[132] For example, depending on the architecture(A:B length ratio) and composition(intermolecular interactions) of the two chains in an AB diblock copolymer, microphase separation leads to many morphologies, including spheres, cylinders, lamellae and bicontinous structures(double-diamond, perforated-lamellar). Recently, Glotzer and coworkers examined the phase behavior of amphiphiles consisting of nanoparticles of various shapes with a finite number and position of surface tethered polymers using Brownian dynamics of coarse grain particle and linear bead-spring chains(FENE potential).[133] **Figure 13** summarizes some of the intriguing possibilities for symmetrically functionalized building blocks. Currently, the synthetic control to make these 'building blocks' with sufficient precision is still being developed. However, significant strides toward the controlled synthesis[134-136] and purification[137] of multivalent nanoparticles, which would enable spatially and numerically defined coupling of polymer chains to the nanoparticle, are continually being reported. For example, Banin and colleagues[134] have demonstrated the single phase synthesis of hybrid metal-semiconductor nanoparticles, such as symmetric two-sided Au tipped CdSe nanorods (nano-dumbbells-NDBs), or asymmetric one-sided Au tipped rods. Dumbbell-like Au-Fe_3O_4 Janus nanoparticles were synthesized using decomposition of $Fe(CO)_5$ on the surface of the Au nanoparticles followed by oxidation in 1-octadecene solvent.[135] Giannelis and coworkers have begun developing synthetic approaches to create monolithic nanoparticle liquids through judicious selection of the organic corona.[138] Roan demonstrated that end-grafted immiscible homopolymers can confer multivalence to nanoparticles, resulting in soft nanopolyhedra with structures identical to those found in small clusters of colloidal microspheres.[139] Krishnamoorti and Matyjaszewski have

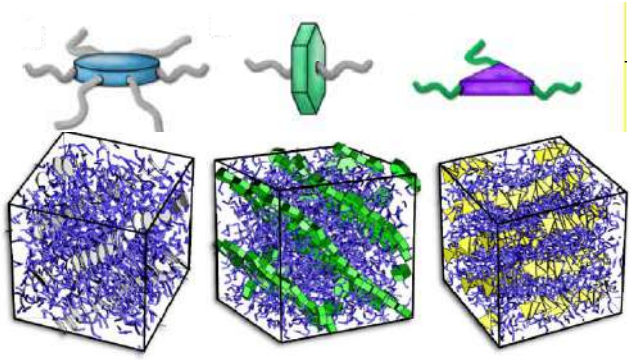

Figure 13. Predicted mesophases of single component melts of structured block nanoparticles by Glotzer *et al.*[133] (left) Hexagonal columnar (cylinder) phase formed from edge-tethered disks. The disks are tilted with respect to the interfacial normal. (middle) Lamellar phase formed from face-tethered hexagonal disks. The disks pack hexagonally within the sheet. (right) Hexagonal columnar phase formed where tethers are attached to the three vertices of a triangular plate. The triangles form a twist about the cylindrical axis.

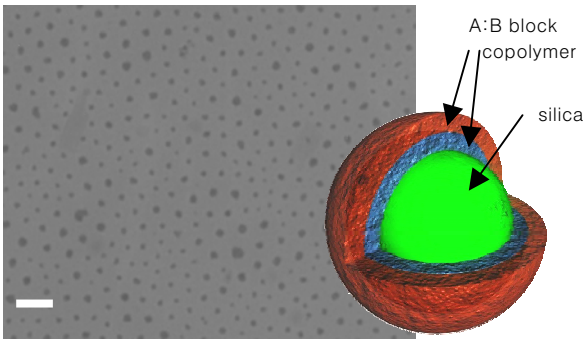

Figure 14. Transmission electron micrograph of a two-dimensional assembly of silica nanoparticles with surface-grafted Poly(methylmethacylate)-Poly(n-butylacrylate)(PMMA-PBA) block copolymer(50:50 PBA: PMMA, MW ~80 K, inner block of PBA).[140] Scale bar is 100 nm.

begun exploring the phase behavior of nanoparticles with macromolecular corona's consisting of surface-grafted, strongly-segregating di-block copolymers, **Figure 14**.[140] In parallel with the synthetic tools, others, such as Landman and co-workers, are beginning to explore the implications of the hard-soft periodicity of these assemblies on their thermal and mechanical properties.[141]

5.3 Nanoparticle-Nanoparticle Systems

Conceptually following blends of nanoparticles with linear chains, combinations of different structured nanoparticles will provide additional routes to even more complex morphologies reminiscent of atomic crystal structures. The possibilities are exemplified by prior work on colloidal crystals and nanoparticle superstructures.

It is noteworthy that even for a simple example of binary mixtures of hard spheres, complex superlattice structures are predicted to occur for specific size ratios and have been observed for classic micron scale colloids.[142-145] Equilibrium phases with stoichiometry of AB_2 and AB_{13} and with upwards of 112 spheres per unit cell can form due solely to entropic considerations, that is due to maximization of the nanoparticle packing density. Murray and coworkers have recently demonstrated comparable structures for binary nanoparticle blends, **Figure 15**.[146,147] These recent efforts have also indicated that not only does electrical charges on sterically stabilized nanoparticles determine the super-lattice stoichiometry; additional contributions from van der Waals, steric and dipolar forces also influence the final order and thus can lead to an even greater array of superlattices.

Not all potential structured nanoparticles are spherical however. Non-spherical inter-particle potential can easily be envisioned for multivalent nanoparticles derived from surface tethered polymers.[51,139] As an example, in a series of elegant experiments, Whitesides *et al.*[148,149] have demonstrated clearly the importance of geometrical considerations in the development of long-range structure and have suggested how such structures might be used to engineer nanomaterials. Fraden and coworkers have extensively examined the phase behavior of various shaped viruses includes rods with proteins and polymers.[150,151] Recently M. de Wild *et al.*[152] have used molecules with triangular symmetry (subphtlaocyanine) to produce a number of long range structures on silver surfaces. Recent theoretical and modeling of two dimensional angular particulate systems[153-157] has demonstrated the richness of phase behavior that can occur even in the most simple systems. As previously noted, in all of this work an important question arises, namely; to what degree are the observed phases a consequence of the purely topological and space filling attributes of the particle and to what degree might they be a function of chemical interaction?[158]

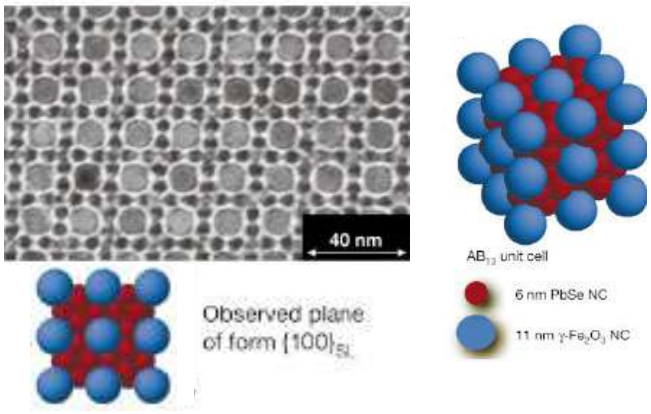

Figure 15. Transmission electron micrograph and sketches of AB_{13} superlattices (isostructural with intermetallic phase $NaZn_{13}$, Space Group 226) of 11-nm γ -Fe_2O_3 and 6-nm PbSe nanocrystals from Murray et al.[146] AB_{13} unit cell depicted is built up of eight cubic subunits.

The process of self-assembly of these complex structures can generally be divided into two broad categories: static and dynamic.[148] Static self-assembly is said to occur when the components are in a global or quasi equilibrium state. The examples discussed above are representative of static self assembly. While an energy burden may occur to enter the static state, energy dissipation is not required to maintain this state. Static equilibrium is most often seen in crystalline assemblies of proteins, colloids, or mesoparticles. In contrast, dynamic self-assembly requires a continual infusion of energy to maintain its quasi-equilibrium state. For instance cellular mitosis[159] and circadian rhythms[160] may be viewed as a form of dynamic self-assembly. In this regard it is intriguing to note that "simple" diffusion which is governed by a first order differential equation can give rise to complex patterns when two components with differing diffusion rates exist within the same system.[161] Nanoparticle Pickering emulsions discussed above (and other examples of DPNDs) may be considered an examples of dynamic self assembly.

Overall, there has been comparatively little theoretical and modeling work on the self assembly dynamics of hard space-filling bodies of angular, non-spherical geometry. These dynamics calculations are exceedingly intensive in terms of computer time and it is perhaps for this reason that such studies have only recently been extended to hard space-filling bodies of more complex shape.[157] Frenkel and Maguire[162] and Magda and Tirrel[163] have reported the transport properties of a fluid of infinitely thin hard-line segments. More recently Huthman has used their

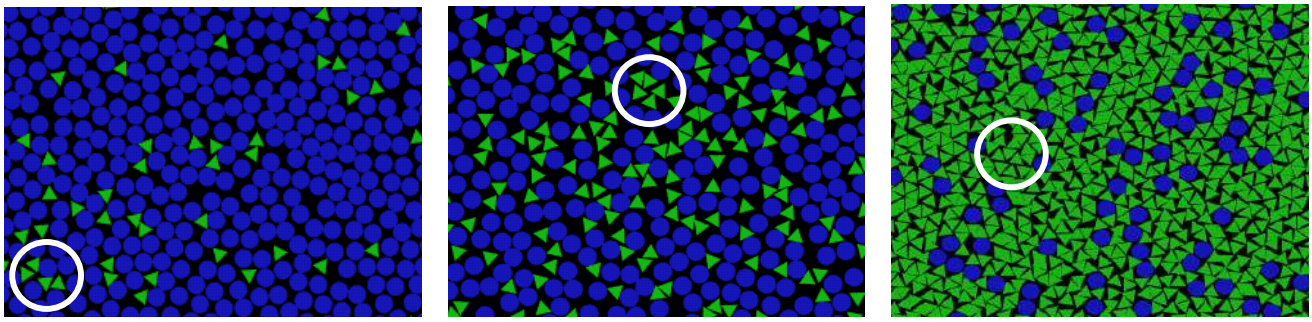

Figure 16. Molecular dynamic simulations of mixtures of hard smooth impenetrable triangles and circles in two dimensions.[166] Even when the mole fraction of the triangles is low (a, χ=0.15) it is noteworthy that the triangles are not randomly distributed on the local scale. As the concentration increases (b, χ=0.375) into the transition region, this tendency to local clustering increases (example circled). At the highest concentration (c, χ=0.80) the triangular fluid forms a liquid quasi-crystalline phase (analogous to Penrose tiling, examples circled) that imposes a non-random local order on the minority circular particles.

approach to simulate granular cooling of hard needles[164] while Yoshimura and Mukoyama[165] have made detailed studies of isolated binary chattering collisions between rods. For example, the hard triangle system undergoes what appears to be a second order phase transition at a packing fraction of ~0.67 and exhibits a clear tendency to form long-lived hexagonal clusters. Similarly in mixtures of circles and triangles, **Figure 16**,[166] there is evidence of clustering of triangular particles at low mole fraction(~0.1) that increase as the system approaches the transition region (0.6).

6. Summary

PNCs have proven that overcoming traditionally antagonistic combinations of properties, while maintaining the manufacturing and processing flexibility inherent to polymers and resins, is possible. For the future, the explosion of functional nanoparticles promises to enable never-before-realized properties to plastics. The framework that is developing to understanding PNC property- morphology correlations implies that the physics and chemistry of these systems parallels many macromolecular and colloidal systems, not just filled polymers. Thus, even more exciting options are anticipated to result from the improved control of manufacturing and processing and thus transforming current '*nano-filled systems*' to '*nano- composite systems*.'

The development of a plurality of approaches to control nanoparticle order will inevitably provide solutions to future(and current) manufacturing needs. However, it is difficult to imagine large scale production of PNC components based on many of the discussed techniques. Ultimately, complete hierarchal control of the morphology will not rely on a single approach, but as with current manufacturing technologies, will depend on the separation of fine and coarse scale control to integrate function and form. Highly ordered nanostructures in the form of sub-micron coatings, fibers and films will be integrated sequentially into larger components, such as commonly done in multi-lamellae film fabrication for food and beverage packaging, in high performance optical coatings for windows and lenses and in fiber-weaving of multifunctional composite structures, just to name a few. Thus true "polymer nanocomposites" when integrated into *material systems* could epitomize the "performance enabled by nano-inside" mantra.

Acknowledgements : The authors are grateful to the Air Force Office of Scientific Research and the Air Force Research Laboratory's Materials and Manufacturing Director for financial support. We would also like to extend our thanks to T. Bunning, Y. Cohen, R. Krishnamoorti, H. Koerner, and L. Drummy for insightful discussions and for providing figures. Finally, RAV is indebted to the Materials Research Laboratory at the University of California, Santa Barbara, as well as E. Kramer, G. Fredrickson and C. Hawker for their outstanding hospitality.

References

1. K. Winey and R. Vaia, eds. *Polymer Nanocomposites,* MRS Bulletin, Materials Research Society, Pittsburgh, PA 2007.
2. Andrew McWilliams, *Nanocomposites, Nanoparticles, Nanoclays, and Nanotubes(NAN021C),* BCC Research, Norwalk, CT, 2006.
3. *Polymer Nanocomposites Create Exciting Opportunities in the Plastics Industry,* Principia Partners, Jersey City, NJ, 2005
4. Ann M. Thayer, *Chemical & Engineering News*, October 16, 2000.
5. Y. Fukushima and S. Inagaki, *Journal of Inclusion Phenomena*, **5**, 473 (1987).

6. Y. Fukushima, A. Okada, M. Kawasumi, T. Kurauchi, and 0. Kamigaito, *Clay Miner.,* **23**, 27 (1988)
7. A. Usuki, M. Kawasumi, Y. Kojima, A, Okada, T. Kurauchi, and 0. J. Kamingaito, *Mater. Res.,* **8**, 1174 (1993).
8. Y. Kojima, A. Usuki, M. Kawasumi, A. Okada, Y. Fukushima, T. Kurauchi, and 0. J. Kamigaito, *Mater. Res.,* **8**, 1185 (1993).
9. R. A. Vaia, H. Ishii, and E. P. Giannelis, *Chem. Mat.,* **5**, 1694 (1993).
10. T. P. Lan and T. J. Pinnavaia, *Chem. Mater.,* **6**, 2216 (1994).
11. E. P. Giannelis, *Adv. Mater.,* **8**, 29 (1996).
12. M. Alexandre and P. Dubois, *Mater. Sci. Eng. Report.,* **28**, 1 (2000).
13. S. S. Ray and M. Okamoto, *Prog. Polym. Sci.,* **2**, 1539 (2003).
14. M. Okamoto, *Polymer/Clay Nanocomposites*, H. S. Nalwa, Editor, American Scientific Publishers, Stevenson Ranch, CA, Vol. 8, p 1 (2004).
15. Erik T. Thostenson, Chunyu Li, and Tsu-Wei Chou, *Composites Science and Technology,* **65**, 491 (2005).
16. L. F. Drummy, H. Koerner, B. L. Farmer, and R. A. Vaia, *CMS Workshop Lecture Series,* Clay Minerals Society, Vol. 14, 2006.
17. S. C. Tjong, *Mater. Sci.Eng. R.,* **53**, 73 (2006).
18. F. Hussain, M. Hojjati, M. Okamoto, and R. E. Gorga, *J. Compos. Mater.,* **40**, 1511 (2006).
19. X.-L. Xie, Y.-W. Maia, and X.-P. Zhou, *Mater. Sci. Eng., R.,* **49**, 89 (2005).
20. M. Moniruzzaman and K. I. Winey, *Macromolecules; (Review),* **39**, 5194 (2006).
21. T. J. Pinnavaia and G. W. Beall J, *Polymer-Clay Nanocomposites*, Wiley, New York, 2001.
22. R. Krishnamoorti and R. A. Vaia, Editor, *Polymer Nanocomposites: Synthesis, Characterization, and Modeling(ACS Symposium Series)* An American Chemical Society Publication, 2001.
23. S. S. Ray and M. Bousmina, *Polymer Nanocomposites and Their Applications American Scientific Publishers*, 2006.
24. Y.-W. Mai and Z.-Z. Yu, Editors, *Polymer nanocomposites, CRC, Woodhead Publishing*, 2006.
25. A. B. Morgan and C. A. Wilkie, Editors, *Flame Retardant Polymer Nanocomposites*, John Wiley & Sons In Press, 2006.
26. L. Drummy and R. Naik, private communication.
27. H. Koerner, R. A. Vaia, W. Liu, M. Alexander, and P. Mirau, *Polymer,* **46**, 4405 (2005).
28. H. Koerner, D. Misra, A. Tan, L. Drummy, P. Mirau, and R. Vaia, *Polymer*, **47**, 3426 (2006).
29. R. A. Vaia and E. P. Giannelis, *MRS Bull*, **26**, 394 (2001).
30. R. A. Vaia and H. D. Wagner, *Materials Today,* **32**, 2004.
31. A. Bansal, H. Yang, C. Li, K. Cho, B. C. Benicewicz, S. K. Kumar, and L. S. Schadler, *Nature Materials*, **4**, 693 (2005).
32. R. Krishnamoorti, R. A. Vaia, and E. P. Giannelis, *Chem Mater.,* **9**, 1728 (1996).
33. F. W. Starr, T. B. Schroeder, and S. C. Glotzer, *Macromolecules*, **35**, 4481 (2002)
34. R. A. L. Jones and R. W. Richards, *Polymers at Surfaces and Interfaces*, Cambridge University Press, Cambridge, UK (1999).
35. R. D. Priestley, C. J. Ellison, L. J. Broadbelt, and J.M. Torkelson, *Science*, **309**, 456 (2005).
36. M. Alcoutlabi and G. B. McKenna, *J. Phys. Condens. Matter,* **17**, (2005).
37. Y. Kojima, A. Usuki, M. Kawasumi, A. Okada, T. Kurauchi, O. Kamigaito, and K Kaji, *Polym. Sci. Pol. Phys.*, **32**, 625 (1994)
38. Y. Kojima, A. Usuki, M. Kawasumi, A. Okada, T. Kurauchi, O. Kamigaito, and K. Kaji, *Polym. Sci. Pol. Phys.*, **33**, 1039 (1995).
39. Brian P. Rice, Chenggang Chen, Larry Cloos, and David Curliss, *SAMPE Journal*, **37**, 7 (2001).
40. A. A. Gusev and M. G. Rozman, *Comput. Theor. Polym. Sci.,* **9**, 335 (1999).
41. A. A. Gusev and H. R. Lusti, *Adv. Mater.,* **13**, 1641 (2001).
42. A. A. Gusev, H. R. Lusti, and P. J. Hine, *Adv. Eng. Mater.,* **4/12**, 927 (2002).
43. N. Sheng, M. C. Boyce, D. M. Parks, G. C. Rutledge, J. I. Abes, and R. E. Cohen, *Polymer,* **45**, 487 (2004).
44. G. A. Buxton and A. C. Balazs, *J. Chem. Phys.,* **117**, 7649 (2002).
45. T. Liu and S. Kumar, *Nano Lett.,* **3/5**, 647 (2003).
46. X. Zheng, M. Gregory Forest, R. Vaia, M. Arlen, and R. Zhou, manuscript in preparation 2006.
47. O. Masala and R. S. Annu, *Rev. Mater. Res.,* **34**, 41 (2004).
48. B. L. Cushing, V. L. Kolesnichenko, and C. J. O'Connor, *Chem. Rev.,* **104**, 3893 (2004).
49. N. Zheng, J. Fan, and G. D. Stucky, *J. Am. Chem. Soc.,* **128**, 6550 (2006).
50. Y.-W. Jun, J.-W. Seo, S. J. Oh, and J. Cheon, *Coordination Chemistry Reviews,* **249**, 1766 (2005).
51. R. R. Naik, S. E. Jones, C. J. Murray, J. C. McAuliffe, R. A. Vaia, and M. O. Stone, *Adv. Functional Meteriasls,* **14**, 25, (2004).
52. C. J. Murphy, T. K. Sau, A. M. Gole, C. J. Orendorff, J. Gao, L. Gou, S. E. Hunyadi, and T. Li, *J. Phys. Chem. B,* **109**, 13857 (2005).
53. A.-C. Grillet, S. Brunel, Y. Chevalier, S. Usoni, V. A.-Alex, and J. Allemand, *Polym. Int.,* **53**, 569 (2004).
54. Hao Fong, Richard A. Vaia, Jeffrey H. Sanders, Derek Lincoln, Andrew J. Vreugdenhil, W. Liu, J. Bultman, and C. Chen, *Chem. Mater.,* **13**, 4123 (2001).
55. H. Fong, W. Liu, C-S. Wang, and R. A. Vaia, *Polymer,* **43**, 775 (2002).
56. S. Pavlikova, R. Thomann, P. Reichert, R. Mulhaupt, A. Marcincin, and E. Borsig, *J. Appl. Polym. Sci.,* **89**, 604 (2003).
57. B. Vigolo, A. Pénicaud, C. Coulon, C. Sauder, R. Pailler, C. Journet, P. Bernier, and P. Poulin, *Science*, **290**, 1331 (2003)
58. S. Kumar, T. D. Dang, F. E. Arnold, A. R. Bhattacharyya, B. G. Min, X. Zhang, R. A. Vaia, R. A. Park, W. W. Adams, R. H. Hauge, R. E. Smalley, S. Ramesh, and S. Willis, *Macromolecules*, **35**, 9039 (2002).
59. T. E. Dirama and L. A. Goettler, *Materials and Manufacturing Processes,* **21**, 199 (2006).
60. J. W. Cho and D. R. Paul, *Polymer*, **42**, 1083 (2001).
61. R. Krishnamoorti and K. Yurekli, *Curr. Opin. Coll. Interface. Sci.,* **6**, 464 (2001).
62. G. Schmidt, A. I. Nakatani, P. D. Butler, A. Karim, and C. C.

Han, *Macromolecules*, **33**, 7219 (2000).
63. H. Koerner, E. Hampton, D. Dean, Z. Turgut, L. Drummy, P. Mirau, and R. Vaia, *Chem. Mater.,* **17**, 1990 (2005).
64. M. J. Casavant, D. A. Walters, J. J. Schmidt, and R. E. Smalley, *J. Appl. Phys.,* **93**, 2153 (2003).
65. H. Koerner, J. . Jacobs, . W. Tomlin, J. Busbee, and R. A. Vaia, *Adv. Materials,* **16**, 297 (2004).
66. Y. Lvov, K. Ariga, I. Ichinose, and T. Kunitake, *Langmuir* **12**, 3038 (1996).
67. M. Olek, J. Ostrander, S. Jurga, H. Möhwald, N. Kotov, K. Kempa, and M. Giersig, *Nano Letters,* 4, 1889 (2004).
68. C. L. T. III and P. Moldenaers, *Annu. Rev. Fluid Mech.,* **34**, 177 (2002).
69. S.-Y. Park, Y.-H. Cho, and R. A. Vaia, *Macromolecules*, **38**, 1729 (2005).
70. Y. Cohen, Albalak, J. R. Dair, J. Benita, M. S. Capel, and L. E. Thomas, *Macromolecules*, **33**, 6502 (2000).
71. Q. Lei and K. I. Winey, *Macromolecules*, **33**, 851 (2000).
72 J. P. A. Fairclough, C. L. O. Salou, A. J. Ryan, I. W. Hamley, C. Daniel, W. I. Helsby, C. Hall, R. A. Lewis, A. J. Gleeson, G. P. Diakun, and G. R. Mant, *Polymer,* **41**, 2577 (1999).
73. V. T. O'Brien and M. E. Mackay, **46**, 557 (2002).
74. T. C. Halsey, *Science*, **258**, 761 (1992).
75. F. D. Goncalves, J.-H. Koo, and M. Ahmadian, *The Shock and Vibration Digest*, **38**, 203 (2006).
76. R. Westermeier, *Electrophoresis in Practice: A Guide to Methods and Applications of DNA and Protein Separations*, John Wiley & Sons, 2005.
77. M. P. Hughes, *Nanotechnology*, **11** 124 (2000).
78. M. D. Morariu, N. E. Voicu, E. Schäffer, Z. Lin, T. P. Russell, and U. steiner, *Nat. Mater,* **2**, 48 (2003).
79. D. Kim and W. Lu, *Phys Rev. B.,* **73**, 35206 (2006).
80. P. R. C. Gascoyne and J. Vykoukal, *Electrophoresis*, **23**, 1973 (2002).
81. N. G. Green, A. Ramos, and H. Morgan, *J. Phys. D: Appl. Phys.,* **33**, 632 (2000).
82. B. N. Pal, S. Basu, and D. Chakravorty, *J. Appl. Phys.,* **98**, 84306 (2005).
83. M. J. Casavant, D. A. Walters, J. J. Schmidt, and R. E. Smalley, *J. Appl. Phys.,* **93**, 2153 (2003).
84. C. Park, J. Wilkinson, S. Banda, Z. Ounaies, K. Wise, G. Sauti, P.T. Lillehei, and J. Harrison, *J. Polym. Sci. Pol. Phys.,* **44**, 1751 (2006).
85. H. Koerner, A. Shiota, C. K. Ober and T. Bunning, *Science*, **272**, 252 (1996).
86. R. A. Vaia, C. L. Dennis, L. V. Natarajan, V. P. Tondiglia, D. W. Tomlin, and T. J. Bunning, *Adv. Mater,* **13**, 1570 (2001).
87. R. Jakubiak, D. P. Brown, F. Vatansever, V. P. Tondiglia, L. V. Natarajan, D. W. Tomlin, T. J. Bunning, and R. A. Vaia, Proc. SPIE, **4991**, 89.
88. N. Suzuki, Y. Tomita, and T. Kojima, *Appl. Phys. Lett.,* **81**, 4121 (2002).
89. R. Jakubiak, V. P. Tondiglia, L. V. Natarajan, R. L. Sutherland, P. Lloyd, T. J. Bunning, and R. A. Vaia, *Adv. Mater.,* **17**, 2807 (2005).
90. V. P. Tondiglia, L. V. Natarajan, R. L. Sutherland, D. Tomlin, and T. J. Bunning, *Adv. Mater.,* **14**, 187 (2002).
91. Y. S. Lipatov, *Prog. Polym. Sci.,* **27**, 1721 (2002).
92. J. S. Hong, H. Namkung, K. H. Ahn, S. J. Lee, and C. Kim, *Polymer* **47**, 3967 (2006).
93. M.Y. Gelfer, H. H. Song, L. Liu, B. S. Hsiao, and B. Chu, *J. Polym. Sci, Part B: Polym. Phys.,* **41**, 44 (2003).
94. S. S. Ray, S. Pouliot, M. Bousmina, and L. A. Utracki, *Polymer*, **45**, 8403 (2004).
95. H. Wolfgang, *Angew. Chem. Int. Ed.,* **44**, 5172 (2005).
96. P. B. Bernard and H. C. John, *Langmuir*, **18**, 1270 (2002).
97. Y. Lin, H. Skaff, T. Ermick, A. D. Dinsmore, and T. P. Russell, *Science*, **299**, 226 (2003).
98. H. Duan, D. Wang, D. G. Kurth, and H. Mohwald, *Angew. Chem.,* **116**, 5757 (2004).
99. H. Duan, D. Wang, N. S. Sobal, M. Giersig, and D. G. Kurth, *Nano Lett.,* **5**, 949 (2005).
100. N. P. Ashby and B. P. Binks, *Phys. Chem. Chem. Phys.,* **2**, 5640 (2000).
101. K. Y. Lee, M. Kim, J. Hahn, J. S. Suh, I. Lee, K. Kim, and S. W. Han, *Langmuir*, **22**, 1817 (2006).
102. D. J. Voorn, W. Ming, and A. M. V. Herk, *Macromolecules*, **39**, 2137 (2006).
103. E. R. Zubarev, J. Xu, A. Sayyad, and J. D. Gibson, *J. Am. Chem. Soc.,* **128**, 4958 (2006).
104. E. Glogowski, J. He, T. P. Russell, and T. Emrick, *Chem. Commun.,* 4050 (2005).
105. C. Tsitsilianis, D. Voulgaris, M. Stepanek, K. Podhajecka, K. Prochazka, Z. Tuzar, and W. Brown, *Langmuir*, **16**, 6868 (2000).
106. N. Hadjichristidis, S. Pispas, M. Pitsikalis, H. Iatrou, and C. Vlahos, *Advances in Polymer Science,* **142**, 71 (1999).
107. J. Barker and D. Henderson, *J. Chem. Phys,* **47**, 2856.
108. C. Gray K. Gubbins, *Theory of Molecular Fluids,* Oxford University Press, Vol. 1, 1984.
109. J. Rowlinson and F. Swinton, *Liquids and Liquid Mixtures,* 3rd edition, Butterworths, London, 1982.
110. Q. Wang, *J. Chem Phys,* **116**, 9120 (2002).
111. P. J. Flory and A. Abe, *Macromolecules*, **11**, 1119 (1978).
112. L. Onsager, *Ann. NY. Acad. Sci.,* **51**, 627 (1949).
113. P. G. de Gennes and J. Proust, *The Physics of Liquid Crystals,* 2nd edition, Oxford University Press, Oxford, 1993.
114. J. B. Hooper and K. S. Schweizer, *Macromolecules*, **39**, 5133 (2006).
115. Y.-L. Chen and K. S. Schweizer, *J. Phys. Chem. B,* **108**, 6687 (2004).
116. L. Zhao, Y.-G. Li, C. Zhong, and J. Mi, *J. Chem. Phys.,* **124**, 144913, (2006).
117. M. E. Mackay, A. Tuteja, P. M. Duxbury, and C. J. Hawker, *J. Disper. Sci. Technol.,* **311**, 1740 (2006).
118. V. V. Ginzburg and A. C. Balazs, *Adv. Mater.,* **12**, 1805 (2000).
119. V. V. Ginzburg, C. Singh, and A. C. Balazs. *Macromolecules,* **33**, 1089 (2000).

120. J.-C. P. Gabriel and P. Davidson *Top. Curr. Chem.,* **226**, 119 (2003).
121. J. C. P. Gabriel, F. Camerel, B. J. Lemaire, H. Desvaux, P. Davidson, and P. Batail, *Nature*, **413**, 504 (2001).
122. P. Davidson, P. Batail J. C. P. Gabriel, J. Livage, C. Sanchez, and C. Bourgaux, *Prog. Polym. Sci.,* **22**, 913, (1997).
123. L.-S. Li, M. Marjanska, G. H. J. Park, A. Pines, and A. P. Alivisatos, *J. Chem. Phys.,* **120**, 1149 (2004).
124. V. A. Davis, L. M. Ericson, A. Nicholas G. Parra-Vasquez, H. Fan, Y. Wang, V. Prieto, J. A. Longoria, S. Ramesh, R. K. Saini, C. Kittrell, W. E. Billups, W. W. Adams, R. H. Hauge, R. E. Smalley, and M. Pasquali, *Macromolecules*, **37**, 154 (2004).
125. B. J. Kim, J. J. Chiu, G.-R. Yi, D. J. Pine, and E. J. Kramer *Adv. Mater.,* **17**, 2618 (2005).
126. Y. Lin, A. Bocker, J. He, K. Sill, H. Xiang, C. Abetz, X. Li, J. Wang, T. Emrick, S. Long, Q. Wang, A. Balazs, and T. P. Russell, *Nature,* **434**, 55 (2005).
127. Y.-H. Ha, Y. Kwon, T. Breiner, E. P. Chan, T. Tziane-topoulou, R. E. Cohen, M. C. Boyce, and E. L. Thomas, *Macromolecules*, **38**, 5170, (2005).
128. B. Kim, J. Bang, C. J. Hawker, and E. J. Kramer, *Macromolecules*, **39**, 4108 (2006).
129. S. W. Sides, B. J. Kim, E. J. Kramer, and G. H. Fredrickson *Phys. Rev. Lett.,* **96**, 250601-4 (2006).
130. B. Kim, C. J. Hawker, G. H. Fredrickson, and E. J. Kramer, manuscript in preperation.
131. M. W. Matsen and F. S. Bates, *J. Chem. Phys.,* **106**, 2436, (1997).
132. A. M. Donald, A. H. Windle, and S. Hanna, *Liquid Crystalline Polymers*, Cambridge University Press, 2nd edition, 2006.
133. S. C. Glotzer, M. A. Horsch, C. R. Iacovella, Z. Zhang, E. R. Chan, and X. Zhang, *Science*, **10**, 287 (2005).
134. T. Mokari, C. G. Sztrum, A. Salant, E. Rabani, and U. Banin, *Nature Materials,* **4**, 855 (2005).
135. H. Yu, M. Chen, P. M. Rice, S. X. Wang, R. L. White, and S. Sun, *Nano Letters,* **5**, 379 (2005).
136. S. J. Hurst, E. K. Payne, L. Qin, and C. A. Mirkin, *Angew. Chem. Int. Ed.,* **45**, 2672 (2006).
137. R. Levy, Z. Wang, L. Duchesne, R. C. Doty, A. I. Cooper, M. Brust, and D. G. Fernig, *Chem. Bio. Chem.,* **7**, 592 (2006).
138. A. B. Bourlinos, R. Herrera, N. Chalkias, D. D. Jiang, Q. Zhang, L. A. Archer, and E. P. Giannelis, *Adv. Mater.,* **17**, 234 (2005).
139. J.-R. Roan, *Phys. Rev. Lett.,* **96**, 248301 (2006).
140. Krishnamoorti and K. Matyjaszewski, 2006 private communication.
141. U. Landman and W. D. Luedtke, *Faraday Discuss.,* **125**, 22 (2004).
142. P. Bartlett, R. R. Ottewell, and P. N. Pusey, *Phys. Rev. Letters.,* **68**, 3801 (1992).
143. E. Trizac, M. D. Eldridge, and P. A. Madden, *Molecular Physics,* **90**, 675 (1997).
144. M. J. Murray and J. V. Sanders, *Phil. Mag.,* **42**, 721 (1980).
145. M. D. Eldridge, P. A. Madden, and D. Frenkel, *Nature,* **365**, 35 (1993).
146. F. X. Redl, K.-S. Cho, C. B. Murray, and S. O'Brien, *Nature*, **55**, 439, (2006).
147. F. X. Redl, K.-S. Cho, C. B. Murray, and S. O'Brien, *Nature,* **423**, 968 (2003).
148. G. Whitesides and B. Gryzbowski, *Science,* **295**, 2418 (2002).
149. C. Mao, V. Thalladi, D. Wolfe, S. Whitesides, and G. Whitesides, *J. Am. Chem. Soc.,* **124**, 14508 (2002).
150. S. Fraden, "Phase transitions in colloidal suspensions of virus particles", In M. Baus, L.F. Rull, and J. P. Ryckaert, edition, "Observation, Prediction, and Simulation of Phase Transitions in Complex Fluids", *NATO ASI Series C*, Vol 460, pp. 113-164, Kluwer Academic Publishers (1995).
151. Z. Dogic, D. Frenkel, and S. Fraden, *Phys Rev E,* **62**, 3925, 2000.
152. M. de Wild, S. Berner, H. Sizuki, H. Yanagi, D. Schlettwein, S. Ivan, A. Baratoff, and H.-J. Güntherodt, *Chem. Phys. Chem.,* **10**, 881 (2002).
153. K. Wojciechowski and D. Frenkel, *Comp. Meth. Sci.Tech.,* **10**, 235 (2004).
154. T. Schilling, S. Pronk, B. Mulder, and D. Frenkel, *Phys. Rev. E,* **71**, 2005, p 036138.
155. M. Bates and D. Frenkel, *J. Chem. Phys.,* 112, 10034 (2000).
156. Y. M.-Raton, E. Velasco, and L. Mederos, *Phys Rev E,* **72**, 031703, 2005.
157. M. Benedict and J. F. Maguire, *Phys. Rev. B.,* **70**, 174112 (2004).
158. J. Herzfeld, *Acc. Chem. Res.,* **V29**, 33 (1996).
159. J. Shapiro, *Annu. Rev. Microbiol*, **52**, 81 (1998).
160. S. S. Sync, *Nature, and Daily Life*, Hyperion, 2003.
161. T. Shinbrot and F. Muzzio, *Nature*, **410**, 251 (2001).
162. D. F. J. Maguire, *Molecular Physics*, **49**, 503 (1983).
163. J. Magda, H. Davies, M. Tirrell, *J. Chem. Phys.,* **85**, 6674 (1986).
164. T. Aspelmeier, M. Huthmann and A. Zeppelius, *Granular Gases,* T. Poschel and S. Herding, Editors ,Springer 2001.
165. Y. Mukoyama and A. Yoshimura,. *Phys A: Math Gen,* **30**, 6667 (1997).
166. M. Benedict, J. Elliott, and J. F. Maguire, personal communication.